Yu.M. Solonin, O.Z. Galij, K.O. Graivoronska, A.V. Sameljuk, S.S. Petrovska

The Influence of Air Exposition of the Zr-Mn-Cr-Ni-Al Alloy on Cycle Life

Frantsevich Institute for Problems of Material Sciences, NAS Ukraine 3, Krzhyzhanovsky str., Kyiv, 03680, Ukraine

It was found by scanning electron microscopy method that the $ZrMn_{0.5}Ni_{1.2}Cr_{0.18}A_{0.1}$ alloy has a dendritic structure, and the shooting of a typical section of the surface of the metalographic sample in characteristic radiation determined its chemical heterogeneity.

The X-ray diffraction method has found that the C_{15} and C_{14} are the main phases of the alloy. In addition, the alloy contains $Ni_{10}Zr_7$ and $Ni_{11}Zr_9$ secondary phases.

The method of potentiometric cycling has established that the air exposition of $ZrMn_{0.5}Ni_{1.2}Cr_{0.18}A_{0.1}$ alloy powder results in an increase in the electrochemical stability of the electrodes pressed from this powder and causes a significant increase of their cycle life. It is important that the cycle life of the AB_2 alloy doped simultaneously with chromium and aluminum increased. Such doping is usually carried out in order to increase the cycle life due to the creation of hydrogen penetrating stable oxide films.

Alloys with the same content of the $Ni_{10}Zr_7$ phase have the same activation rate of the initial electrodes. The increase in the secondary phase of $Ni_{10}Zr_7$ leads to an improvement in the kinetics of hydrogenation of the initial electrode. Exposition in air of a powder of an alloy with an increased content of the $Ni_{10}Zr_7$ phase does not accelerate the kinetics of hydrogenation, but it leads to a significant improvement in its cyclic stability. By reducing the amount of $Ni_{10}Zr_7$ phase, the improvement of kinetics of hydrogenation occurs as a result of the exposition of the powder of the alloy in the air.

The mechanism of origination and distribution of corrosion of the alloy without and with exposition in air for 7 and 15 days with subsequent aging in 30% solution KOH is the same. According to investigations, corrosion of the material originates on the interphase surface and begins to spread along it, indicating its pitting nature, and the surface of the pitting itself has the form of flake.

Keywords: Zr-alloy, hydrogenation, exposition in air.

Introduction

Problems with the environment make finding alternative sources of energy relevant. Solving this problem is possible due to the use of hydrogen as a fuel and energy carrier. The storage and transport of hydrogen in pure form is a complicated and dangerous process, so the scientists' discovery of the ability of intermetallic compounds to sorption - desorption of hydrogen has led to the creation of a "metal-hydrogen" system as a reliable and safe storage facility [1-3]. Since the discovery of IMC, many devices, including storage batteries, have been developed and proposed for practical use on their basis. In recent decades, nickel-metal hydride (NMH) batteries are becoming increasingly popular. Promising materials for nickel-metal hydride accumulators are alloys of type AB_5, AB_2, AB_{3-4} [4-5].

In this paper, an alloy of AB_2 type (Laves phase) is chosen for the study. Among the main disadvantages, which complicate their wider application is the need for activation and insignificant cycle life when working in alkaline electrolyte, which reduction is possible due to mechanical destruction as a consequence of the significant volume effect of the reaction of hydrogenation-dehydrogenation and corrosion.

As a result of numerous studies, it has been found that increase of the cycle life of zirconium alloys is possible during their processing in fluoride-containing solutions when doping in order to reduce the volume effect of the hydrogenation and doping in order to create hydrogen penetrating stable oxide films [6-8].

Our research has found that increase of the cycle life of zirconium alloy ZrMnCrNiV is also possible when it exposed to air in the form of powder or ingot [9-10]. Exposition of the alloy in the air leads to its metered oxidation, mainly from the surface, and contributes to the fact that the electrode, pressed from the already partially

Yu.M. Solonin, O.Z. Galij, K.O. Graivoronska, A.V. Sameljuk, S.S. Petrovska

oxidized powder, during hydrogenation-dehydrogenation is more resistant to further oxidation in the electrolyte, resulting in increase of cyclic stability. In this paper we present the results of corrosion-electrochemical studies of air-exposed powder of ZrMnCrNiAl alloy.

I. Experimental details

The ZrMnCrNiAl alloy with weight 7, 15, and 25 g (alloy No. 1, 2 and 3, respectively) was obtained by the argon-arc melting method. The composition of the alloy is given in Table 1.

The alloy samples were validated by X-ray diffraction analysis using DRON-3M with Bragg-Brentano focusing. The voltage and current on the X-ray tube were 30 kV and 25 mA, respectively. The recording was carried out in Cu $K\alpha$ - monochromatic radiation in the range of angles 2Θ from 30 to 80° with a scanning step of 0.05°, the integral action time was 10 seconds. A single crystal of graphite was used as a monochromator on a secondary beam.

Powder morphology, structure, chemical inhomogeneity and the mechanism of corrosion of the alloy were examined by scanning electron microscopy and X-ray microanalysis using the microanalyzer "Superprobe-733" (JEOL, Japan). The morphology was recorded in secondary electrons (SEI), structures were recorded in reflected electrons (BEI). The investigations were carried out with an accelerating voltage of 25 kV and a beam current of $1x10^{-10}$ A for electron microscopic studies and $2x10^{-7}$A for X-ray spectral studies. Working vacuum was $1x10^{-5}$ atm.

Table1

Composition of Zr-containing alloy

Formula composition			
Zr -1	Mn – 0.5	Ni – 1.2	Cr – 0.180	Al 0.1
Weight % of components in the alloy			
Zr – 45.34	Mn– 13.66	Ni – 35.01	Cr – 4.65	Al – 1.34

Fig. 1. The typical view of the surface of metalographic sample of $ZrMn_{0.5}Ni_{1.2}Cr_{0.18}Al_{0.1}$ alloy (x 300, BEI).

The voltage-current characteristics were studied by the method of cyclic voltamperometry (CVA). Recording of potentiodynamic polarization curves from the stationary potential of the electrode to a potential of -1.6V (forward stroke) and from -1.6V to -0.6 V (reverse stroke) relative to the oxide-mercury reference electrode in a three-electrode cell with separated electrode spaces in a 30 % KOH solution using the PI-50-1.1 potentiostat at a potential sweep speed of 2 mV/s. Measurements were carried out at a temperature of 20 ± 2^0 C.

The cycle life of the samples was studied by cycling in the galvanostatic mode in a two-electrode cell on a 4-channel automatic module equipped with nonvolatile memory, which provides the restoration of experimental data during repeated program launches. The measurements were carried out at a temperature of 20 ± 2^0C in a 30% solution of KOH. The electrode of the Ni/Ni (OH)$_2$ system served as the counter electrode. The charge of the electrodes was conducted with a current of 50 mA for 1.5 hours, a discharge with a current of 5 mA until a potential difference of 0.8 V was reached.

Exposition of the alloy in the air means aging of powders in laboratory conditions in the open air and natural moisture, in which changes of powders as a result of processes of hydrolysis, oxigenolysis and hydrogenolysis are possible.

II. Results and discussion

To determine the structure of the $ZrMn_{0.5}Ni_{1.2}Cr_{18}Al_{0.1}$ alloy, the shooting of the surface of its metalographic sample was performed. It is established that the material has a dendritic structure and consists of several phases, which differ in contrast (Fig. 1). The light phase corresponds to a higher average atomic weight, and dark phase corresponds to lesser one.

Shooting of the typical section of the metalographic sample surface in the characteristic radiation of all the elements included in the material (Fig. 2) has been taken to determine its chemical heterogeneity. According to the results of the survey, it was concluded that the lighter phase is enriched with Ni and Zr, which, according to the X-ray diffraction analysis, the equilibrium diagram and the calculation of the average atomic weights, corresponds to the phases Zr_7Ni_{10} and Zr_9Ni_{11} and, possibly, ZrNi, Zr_3Al (average atomic weighing 72-75). The darker phases correspond to $ZrMn_2$, $ZrCr_2$, $ZrNi_3$, (average atomic weight 65-67), and possibly Zr_3Al_3, Zr_2Al (average atomic weight - 59 and 70, respectively). Due to the closeness of the atomic weights Ni, Mn and Cr (58.71 , 54.94 and 52.01, respectively), it is impossible to visually distinguish the phases in details.
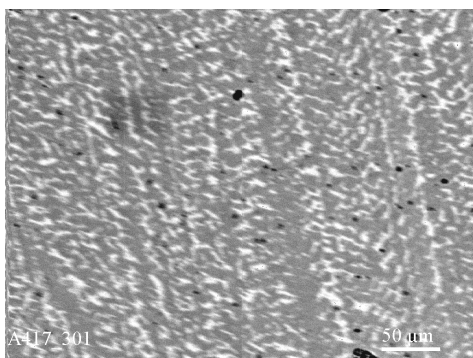
Scanning electron microscopy study of the alloy morphology was made after the grinding of the alloy into particles of <100 μm. It was found that all particles, irrespective of their size, were of irregular shape (Fig. 3).

X-ray diffractometric method has been applied to investigate three $ZrMn_{0.5}Ni_{1.2}Cr_{0.18}Al_{0.1}$ alloys (№ 1, 2 and 3 weighing 7, 15 and 25 g, respectively). The received X-ray diffraction patterns are shown in Fig. 4.

The processing of diffractograms was carried out by the method of full-profile analysis using the PowderCell 2.4 program, which uses the Rietveld method. The obtained calculation results (R-factor was 6-9%) are shown in tables 2 and 3.
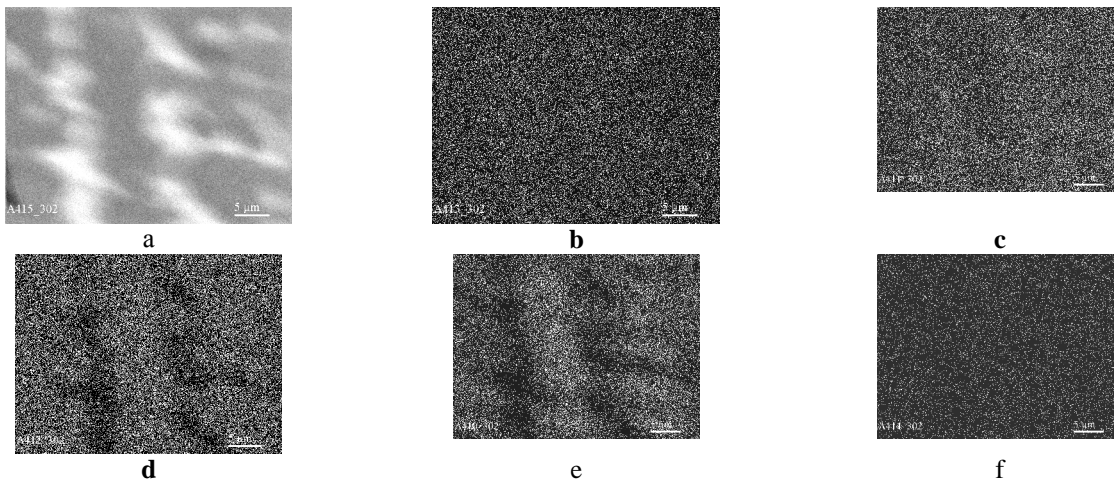
Fig. 2. The distribution of chemical elements in the typical section of the metalographic sample of the $ZrMn_{0.5}Ni_{1.2}Cr_{0.18}Al_{0.1}$ alloy with magnification x3000: a - BEI; b- X-Ray Zr-L_{α} ; c - X-Ray Ni- K_{α}; d- X-Ray Mn-K_{α}; e - X-Ray Cr-K_{α}; f - X-Ray V-K_{α}

Fig. 3. Powder of $ZrMn_{0.5}Ni_{1.2}Cr_{0.18}Al_{0.1}$ alloy with particles size <100 μm (a – x300 SEI, b-x1000 SEI).
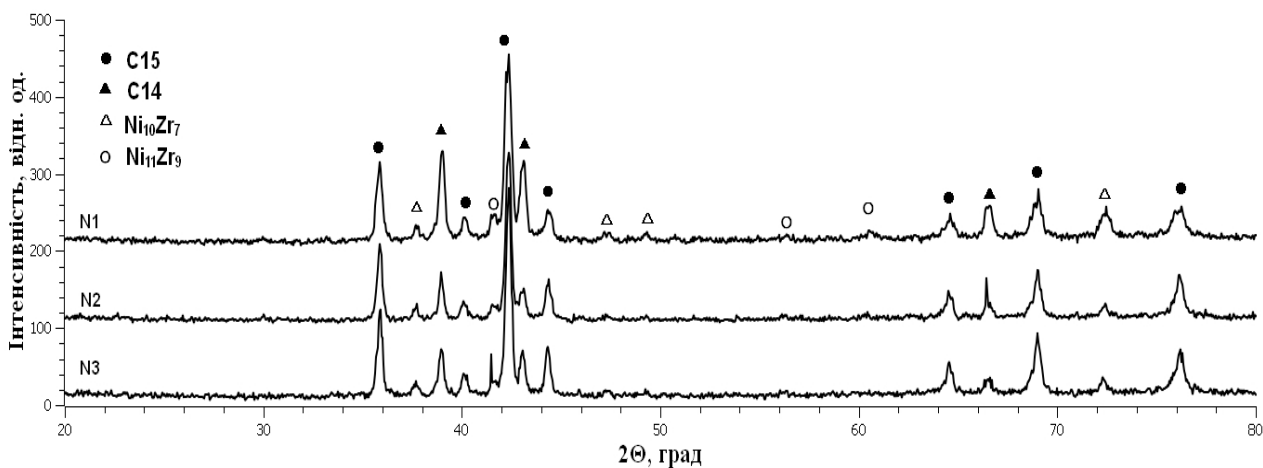
Fig. 4. X-ray diffraction patterns of $ZrMn_{0.5}Ni_{1.2}Cr_{0.18}Al_{0.1}$ alloys № 1-3.

Yu.M. Solonin, O.Z. Galij, K.O. Graivoronska, A.V. Sameljuk, S.S. Petrovska

Table 2

The quantitative phase composition of the $ZrMn_{0.5}Ni_{1.2}Cr_{0.18}Al_{0.1}$ alloy № 1-3 according to calculation results

Main phases	Alloy №1	Alloy №2	Alloy №3
C_{15} (vol%)	25.7	46.6	54.4
C_{14} (vol%)	60.4	29.7	35.7
$Ni_{10}Zr_7$ (vol%)	9.1	9.7	5.0
$Ni_{11}Zr_9$ (vol%)	4.7	14.0	4.8

Table 3

Results of calculation of lattice parameters of the main phases of alloys

Alloy №	AB_2, C_{15}, Fd3m	AB_2, C_{14}, P6₃/mmc		$Ni_{11}Zr_9$, I4/m		$Ni_{10}Zr_7$, Cmca		
	a, nm	a, nm	c, nm	a, nm	c, nm	a, nm	b, nm	c, nm
1	0.70475	0.50006	0.81516	0.96604	0.65656	1.23446	0.91785	0.92352
2	0.70562	0.50030	0.81654	0.96068	0.66586	1.23488	0.92056	0.92293
3	0.70552	0.50037	0.81637	0.97014	0.65466	1.23602	0.92043	0.92247

Table 4

Chemical composition of the $ZrMn_{0.5}Ni_{1.2}Cr_{0.18}Al_{0.1}$ alloy № 1 and 3

	Zr	Mn	Ni	Cr	Al
Alloy №1	45.0	13.6	34.8	4.9	1.3
Alloy №3	45.3	13.6	34.6	4.8	1.3

Table 5

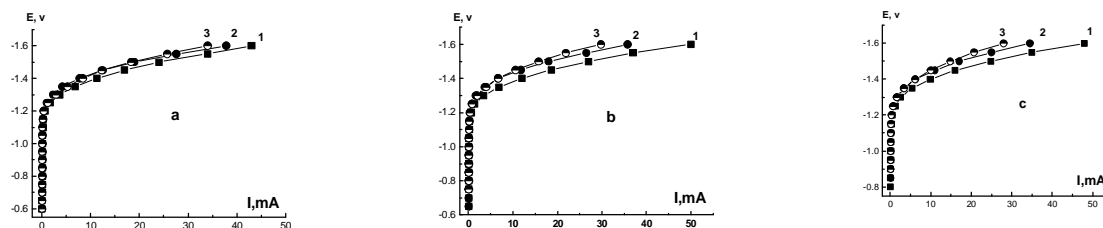Electrodes made from powder of $ZrMn_{0.5}Ni_{1.2}Cr_{0.18}Al_{0.1}$ alloy № 1-3 of different genesis

Alloy №	1			2			3		
Electrode №	1	2	3	4	5	6	7	8	9
Time of exposition in air. days	0	3	15	0	3	10	0	7	15

The main phase of the alloy № 1 is the C_{14} hexagonal phase ($MgZn_2$ type), also this alloy contains a significant amount of C_{15} cubic phase ($MgCu_2$ type) and secondary phases $Ni_{10}Zr_7$ and $Ni_{11}Zr_9$. On the received X-ray diffraction patterns for alloys № 2 and № 3 the main phase is C_{15} cubic phase, the content of the hexagonal phase C_{14} is about 30%, and also secondary phases of $Ni_{10}Zr_7$ and $Ni_{11}Zr_9$ are present. The results of calculation of the lattice parameters of the samples that were validated are presented in Table 2.

The different content of the secondary phase of $Ni_{10}Zr_7$ in the alloys № 1 and 3 is associated with a different rate of its cooling during the melting, since, according to the chemical analysis, the composition of the components of the alloy № 1 and 3 are the same (Table 4).

In the study of electrochemical properties, electrodes made from the powder of $ZrMn_{0.5}Ni_{1.2}Cr_{0.18}Al_{0.1}$ alloy №1 1, 2 and 3 (without and with air exposition) were pressed, as shown in Table 5. Electrodes were prepared by cold pressing in a nickel mesh (diameter of a tablet 8 mm) with additives of polytetrafluoroethylene as a binder. The weight of the alloy in the compacted electrodes was 0.1 g, the compacting pressure was 15 MPa.

To obtain information on the kinetics of hydrogenation, the evaluation of surface activity, and the determination of electrochemical stability of electrodes, the method of cyclic voltamperometry (CVA) was used. From the powder of the $ZrMn_{0.5}Ni_{1.2}Cr_{0.18}Al_{0.1}$ alloy № 1 the electrodes were pressed without and with air exposition for 3, 7, 15 days. Electrochemical behavior of

Fig. 5. Cathode curves of the output electrode (1) and after exposition to air of the powder of the $ZrMn_{0.5}Ni_{1.2}Cr_{0.18}Al_{0.1}$ alloy № 1, days: 2 - 3, 3 -15; a-1 cycle, b- 2 cycle, c - 4 cycle.

the electrodes, pressed from the powder exposed for 7 and 15 days, practically coincides, therefore, in the work the results of research of electrodes from freshly made powder of alloy №1 (initial electrode) and after its exposition in air for 3 and 15 days (electrodes № 2 and 3, respectively) are presented. The activity of the electrodes in the cathode region depending on the time of exposition of the alloy in the air is shown in Fig. 5 (a - c) in the form of a set of curves corresponding to 1, 2 and 4 cycles of potentiometric cycling, as shown in Table 6.

According to Fig. 5, for all electrodes, a wide passivity region from stationary potential to E = -1.2-1.25 V is characteristic in 4 cycles of potentiometric cycling. The highest activity during all studied cycles is shown by the initial electrode № 1 (0 days of exposition). The cathode currents of this electrode in the second cycle, as compared with the first cycle, increase, and those of the electrodes number 2 and 3, on the contrary, decrease. Thus, at a potential of E = -1,6 V, the electrode № 1 in 1 and 2 cycles shows currents of 43.0 and 50.0 mA, an electrode № 2 - of 37.8 and 35.8 mA, an electrode № 3 - of 34.0 and 29.8 mA, respectively.

Different electrochemical stability of the electrodes

Table 6

Change in the value of the cathode current of the fourth cycle relative to the third cycle of forward stroke of cycling of the electrodes № 1 and 2 pressed from the powder of the $ZrMn_{0.5}Ni_{1.2}Cr_{0.18}Al_{0.1}$ alloy № 1

| E, V	Change in the value of the cathode current, mA	
	Electrode number	
	1	2
-1.25	-0.08	+0.02
-1.30	-0.8	-0.03
-1.35	-1.0	+0.1
-1.40	-1.3	+0.1
-1.45	-2.6	+0.3
-1.50	-1.6	+0.3
-1.55	-1.15	0
-1.60	-2.0	-0.1
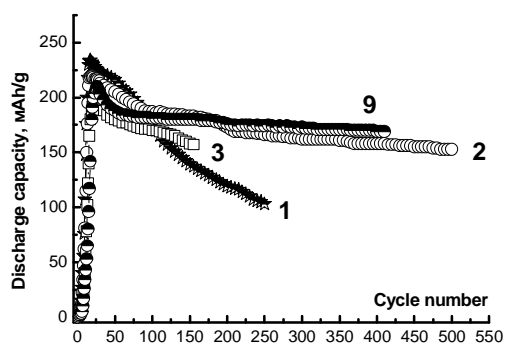
Fig. 6. Dependences of the specific capacity of the electrodes № 1-3, 9 on the number of cycles. The number of the curve corresponds to the number of the electrode according to Table 5.

was revealed during the potentiometric cycling. Therefore an analysis of the behavior of the electrodes of direct / reverse stroke of cycling and from cycle to cycle was performed. Thus, the output electrode № 1 (0 days of exposition) in the first cycle of cycling, according to changes in the value of the cathode current of reverse stroke with respect to the forward stroke, shows the greatest electrochemical stability, which it gradually loses with further cycling. For this electrode in the potential region E = -1.4-1.55V, the currents of the forward and reverse stroke in the first cycle completely coincide. The electrochemical stability of electrodes № 2 and 3 of the forward / reverse stroke of cycling is observed already in the second cycle. As a result a change in the value of the cathode current of these electrodes in reverse stroke in relation to the forward stroke is 3-4 times less compared with the initial electrode № 1.

An analysis of the results of the electrochemical behavior of electrodes during cycle-to-cycle potentiometric cycling shows that for electrodes pressed from air exposed alloy powder (for 3 and 15 days), starting from the third cycle, the values of cathode current change are insignificant in contrast to the initial electrode. According to Table 6, the change in the magnitude of the cathode current of the initial electrode № 1 (0 days of exposition) in the fourth cycle relative to the third cycle of forward stroke of cycling is 9-10 times greater than the corresponding currents of the electrode № 2 (3 days). These data, as well as the abovementioned data, completely correlate with the results of the change in the electrochemical characteristics of electrodes during the galvanostatic cycling (Fig. 8) and in the activation process (Fig. 9). The analysis of the behavior of the electrodes from both the cycle to the cycle and the forward/reverse stroke of the potentiometric cycling shows that the air exposition of the alloy powder results in an increase in the electrochemical stability of the electrodes and causes a significant improvement in their cyclic stability.

On the basis of Fig. 6, the maximum electrochemical capacity shows the initial electrode № 1 (0 days of exposition), which, according to the results of the CVA, has maximal cathode currents in 4 cycles of cycling. Maximum cycle life is demonstrated by electrode № 2 (3 days of exposition). After 500 cycles of hydrogenation-dehydrogenation, the loss of capacity of the given electrode is 26%, and the loss of capacity of the electrode № 1 (0 days of exposition) is 56%. Thus, the electrode № 2, which, according to the CVA, shows better electrochemical stability compared to the electrode № 1 (from cycle to cycle and on the forward / reverse stroke), has increased cyclic stability. The maximum capacity losses of this electrode occur during the first 70 cycles (15%), further they slow down and have a "stepped" character. The behavior of the electrode № 3 (15 days of exposition) during the 150 cycles practically coincides with the behavior of the electrode № 2, except for the maximum capacity.
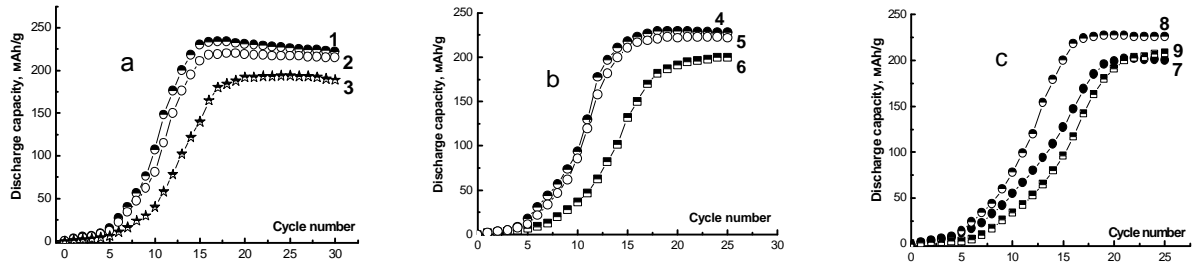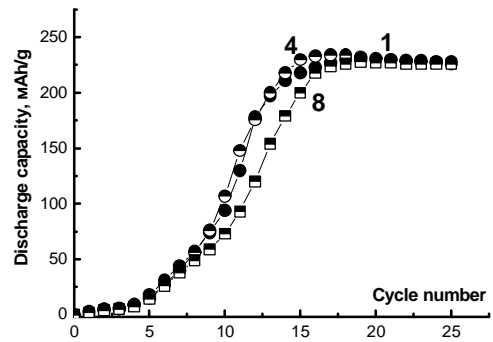
Fig. 7. Dependences of the specific capacity of the electrodes № 1-3 (a), 4-6 (b) and 7-9 (c) on the number of cycles in the activation process. The number of the curve corresponds to the number of the electrode according to Table 5.

The curves of the electrodes № 1-3 of the alloy №1 in the activation process presented in Fig. 7a, show that the air exposition of the powder does not improve the kinetics of hydrogenation. For electrode № 2 (3 days of exposition), it almost coincides with the initial electrode № 1 and deteriorates for the electrode № 3 (15 days of exposition). The maximum capacity of the electrodes № 1 and 2 is achieved during 15 cycles, and the electrode № 3 during 19 cycles. The long air exposition of the alloy № 1 powder leads to a decrease in the maximum capacity. For electrodes № 1 and 2, it is 235 and 225 mAh/g, and for electrode № 3 - 195 mAh/g.

The activation of the electrodes pressed from the powder of the alloy № 2 (Fig. 7b) is similar to the activation of the corresponding electrodes of the alloy № 1. Thus, the activation rate and the maximal achieved capacity of the initial electrode № 4 and pressed from powder exposed in air for 3 days (electrode № 5) practically coincide, and long exposition of powder (for 10 days) deteriorates these characteristics. The initial electrode № 4 has a maximum capacity of 230 mAh/g, which is achieved in 16-17 cycles as compared to 200 mAh/g achieved during 23 cycles by electrode № 6, pressed from powder exposed in air for 10 days.

The activation of the electrodes pressed from the powder of the alloy № 3 differs from the activation of the corresponding electrodes of the alloy № 1 and 2 (Fig. 7c). The initial electrode № 7 of this alloy has a reduced activation rate and a maximum capacity of 203 mAh/g which was achieved during 21 cycles. However, exposition of the powder of the alloy №. 3 in the air for 7 days (electrode № 8) improves the kinetics of hydrogenation. As a result the activation of this electrode and the initial electrodes № 1 and 4 (alloy № 1 and 2, respectively) coincide (Fig. 8). With the long exposition of the powder of the alloy № 3 in air (15 days), the kinetics of hydrogenation deteriorates and the maximum reached capacity (electrode № 9) decreases; however, this electrode shows maximum cycle life (Fig. 6).

It should be noted that alloys №. 1, 2 have the same activation rate of the initial electrodes and the same content of the secondary phase $Ni_{10}Zr_7$ (9.1 and 9.7 vol.%, respectively). According to [11], the $Ni_{10}Zr_7$ phase creates favorable conditions for the hydrogenation reaction on the surface of the main components of the alloy phases of the C_{15} and C_{14} type, the total content of which in the investigated alloy № 1 and 2 is


Fig. 8. Comparison of the dependence of the specific capacity of electrodes №. 1, 4 and 8 on the number of cycles during activation. The number of the curve corresponds to the number of the electrode according to Table 5.
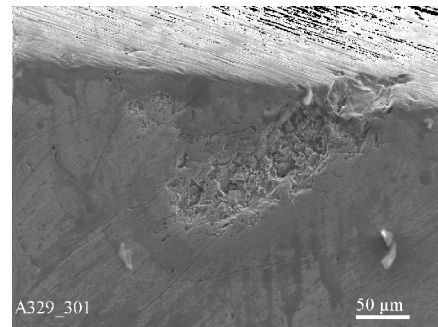

Fig. 9. The surface of the freshly prepared metalographic sample of the $ZrMn_{0.5}Ni_{1.2}Cr_{0.18}Al_{0.1}$ alloy after its aging in 30% KOH solution for 7 days (x300, SEI).

approximately the same. Increased content of the secondary phase of $Ni_{10}Zr_7$ in alloy № 1 and 2 as compared to alloy № 3 improves the kinetics of hydrogenation of the initial electrode and does not affect the activation of the electrodes pressed from the air-exposed powder of the alloy.

To determine the mechanism of corrosion of the alloy $ZrMn_{0.5}Ni_{1.2}Cr_{0.18}$ $Al_{0.1}$ in the KOH solution a scanning electron microscopy method was used. Fig. 9 shows the results of the study of the surface of the freshly prepared metalographic sample of $ZrMn_{0.5}Ni_{1.2}Cr_{0.18}Al_{0.1}$
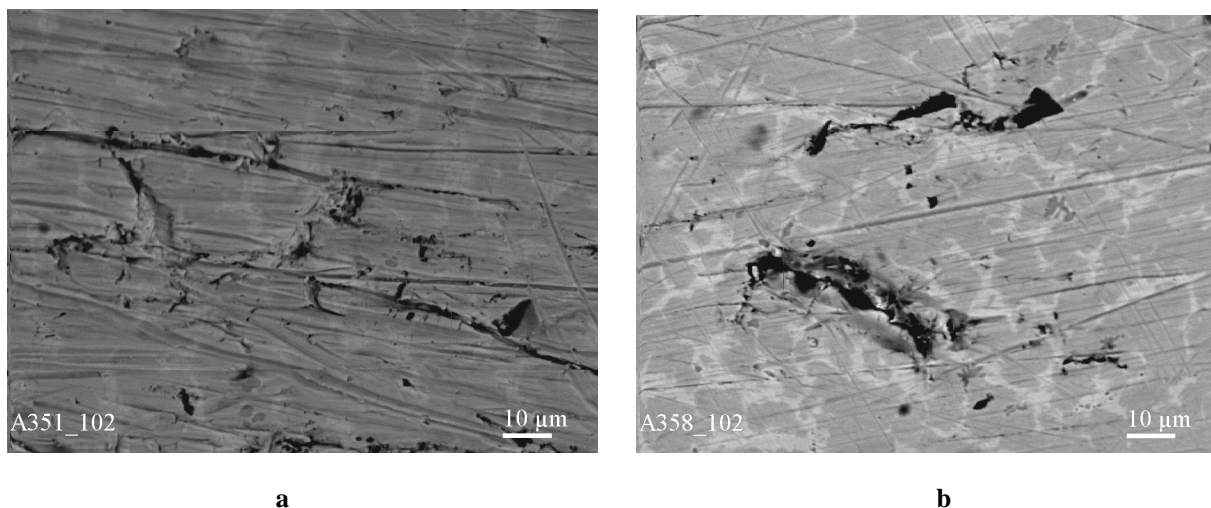
Fig. 10. Distribution of corrosion on the surface of a metalographic sample of $ZrMn_{0.5}Ni_{1.2}Cr_{0.18}A_{0.1}$ alloy without exposition (a) and with expositiom to air for 7 days (b) with subsequent aging in KOH solution for 7 days (a, b) - x1000, BEI.
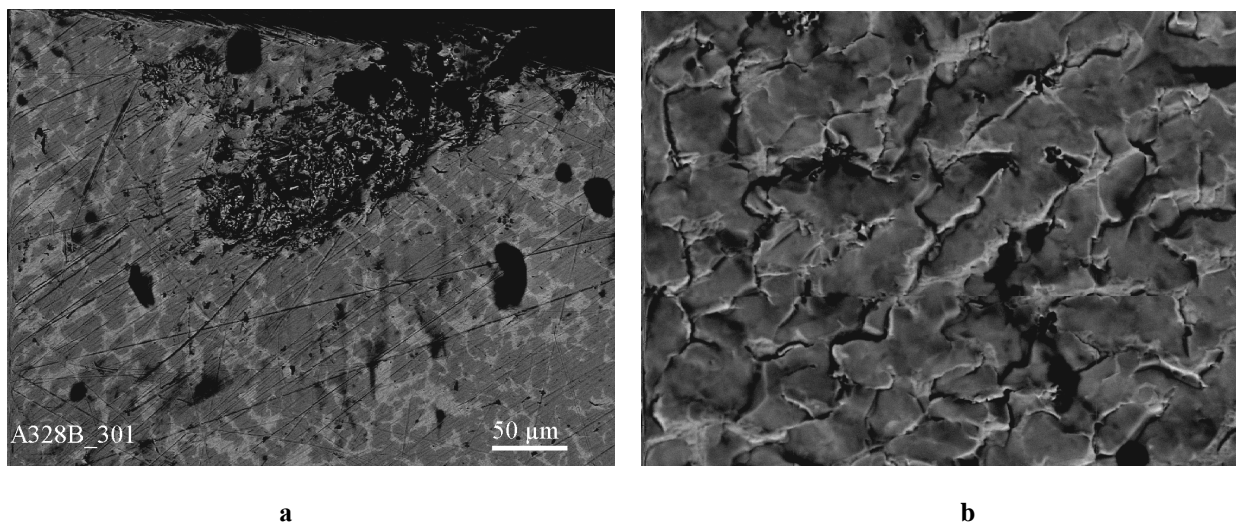
Fig. 11. The viewof the dissection (a- 300, BEI) and surface of pitting (b- 1000, BEI) of $ZrMn_{0.5}Ni_{1.2}Cr_{0.18}A_{0.1}$ alloy.

alloy after its aging in 30% KOH solution for 7 days. The analysis of the surface of the metalographic sample after interaction with the solution shows that it has separate dissolution centers, indicating the local nature of the corrosion of the alloy.

The shooting of the area of corrosion damage on the surface of the metalographic sample in the reflected electrons indicates that the corrosion of the material originates on the interphase surface and begins to spread along it in accordance with equations 1-7 (Fig. 10a).

$$H_2ZrO_3 + H_2O + 4e \rightarrow Zr + 4OH- \qquad E^o = -2,36 \text{ V} \quad (1)$$

$$Al(OH)_3 + 3e \rightarrow Al + 3OH- \qquad E^o = -2.31 \text{ V} \quad (2)$$

$$Mn(OH)_2 + 2e \rightarrow Mn + 2OH- \qquad E^o = -1.55 \text{ B} \quad (3)$$

$$Cr(OH)_2 + 2e^- \rightarrow Cr + 2OH- \qquad E^o = -1.4 \text{ V} \quad (4)$$

$$Cr(OH)_3 + 3e^- \rightarrow Cr + 3OH- \qquad E^o = -1.3 \text{ V} \quad (5)$$

$$CrO_2^- + 2H_2O + 3e^- \rightarrow Cr + 4OH^- \qquad E^o = -1.2 \text{ V} \quad (6)$$

$$Ni(OH)_2 + 2e^- \rightarrow Ni + 2OH^- \qquad E^o = -0.72 \text{ V} \quad (7)$$

In the case of prior air-exposition of the alloy for 7 and 15 days with a subsequent aging in 30% KOH solution, the mechanism of origin and distribution of corrosion remains the same (Fig. 10b).

The dissolution rate of the light phases is less than that of the dark. As a result on the surface of the pitting dissection there is segregation of unsolved light phases (Fig. 11a). The surface of the pitting itself has the form of flakes, which are surrounded by a light phase (Fig. 11b).

Conclusions

It was found by scanning electron microscopy method that the $ZrMn_{0.5}Ni_{1.2}Cr_{0.18}A_{0.1}$ alloy has a dendritic structure, and the shooting of a typical section of the surface of the metalographic sample in characteristic radiation determined its chemical heterogeneity

The X-ray diffraction method has found that the C_{15} and C_{14} are the main phases of the alloy. In addition, the alloy contains $Ni_{10}Zr_7$ and $Ni_{11}Zr_9$ secondary phases.

The air exposition of $ZrMn_{0.5}Ni_{1.2}Cr_{0.18}A_{0.1}$ alloy powder results in an increase in the electrochemical stability of the electrodes pressed from this powder and causes a significant improvement in their cycle life. The electrode, which according to the CVA shows the maximum electrochemical stability (from cycle to cycle and in the forward / reverse stroke), has increased cyclic stability. It is important that the cycle life of the AB_2 alloy doped simultaneously with chromium and aluminum increased owing to air exposition. Such doping is usually carried out in order to increase the cycle life due to the creation of hydrogen penetrating stable oxide films.

Alloys with the same content of the $Ni_{10}Zr_7$ phase have the same activation rate of the initial electrodes. The increase in the secondary phase of $Ni_{10}Zr_7$ leads to an improvement in the kinetics of hydrogenation of the initial electrode. Exposition to air of a powder of an alloy with an increased content of the $Ni_{10}Zr_7$ phase does not accelerate the kinetics of hydrogenation, but it leads to a significant improvement in its cyclic stability. By reducing the amount of $Ni_{10}Zr_7$ phase, the improvement of kinetics of hydrogenation occurs as a result of the exposition of the powder of the alloy in the air.

The mechanism of origination and distribution of corrosion of the alloy without and with exposition in air for 7 and 15 days with subsequent aging in 30% solution KOH is the same. According to investigations, corrosion of the material originates on the interphase surface and begins to spread along it, indicating its pitting nature, and the surface of the pitting itself has the form of flake.

Solonin Yu.M. - professor, academician, doctor of physical and mathematical sciences, director of IPM NAS of Ukraine;
Galij O.Z. - junior research fellow;
Graivoronska K.O. - senior researcher, phd in physics and mathematics;
Sameljuk A.V. - researcher;
Petrovska C.C. - senior researcher, candidate of physical and mathematical sciences.

[1]. Yu. M. Solonin, L.L. Kolomiets, V.V. Skorohod, Alloys-sorbents for Ni-MH current sources (Frantsevich Institute for Problems of Material Sciences, Kyiv, 1993).

[2]. B.E. Paton, ICHMS-2001 (Alushta, 2001), p. 11.

[3]. Yu.M. Solonin, L.L. Kolomiets, S.M. Solonin, V.V. Skorohod, Powder Metallurgy 7, 53 (2003).

[4]. R.V. Denis, V.V. Shtender, I.V. Zavalij, Powder Metallurgy 3-4, 117 (2015).

[5]. F.E. Lynk, J. Less-common Metals. 172-174 (1-2), 943 (1991).

[6]. L. Li, W. Wang, X. Fan, X. Jin, H. Wang, Y. Lei, Q. Wang, L. Chen, J. Hydrogen Energy 32, 2434 (2007).

[7]. H. Pan, R. Li, M. Gao, Y. Liu, Q. Wang, J. Alloys Compd. 404-406, 669 (2005).

[8]. L. Yongquan, Y. Xiaoguang, W. Jing, W. Qidong, J. Alloys Compd. 231, 573 (1995).

[9]. Yu.M. Solonin, O.Z. Galiy, K.O. Grajvoronska, O.Yu. Khyzhun, Physical-chemical mechanics of materials 2, 24 (2017).

[10]. Yu.M. Solonin, O.Z. Galiy, K.O. Grajvoronska, V.A. Lavrenko, Powder Metallurgy 9-10, 101 (2017).

[11]. M.V. Karpets, O.A. Gniteskyy, S.V. Sirichenko, Yu.M. Solonin, ICHMS-2001 (Alushta, 2001), p. 108.

Ю.М. Солонін, О.З. Галій, К.О. Грайворонська, А.В. Самелюк, С.С. Петровська

**Вплив витримки на повітрі сплаву Zr-Mn-Cr-Ni-Al
на циклічну стійкість**

Інститут проблем матеріалознавства ім. І.М. Францевича НАН України3, вул. Кржижанівського, Київ, 03680, Україна, o.galiy87@gmail.com

Методом растрової електронної мікроскопії встановлено, що сплав $ZrMn_{0.5}Ni_{1.2}Cr_{0.18}A_{0.1}$має дендритну структуру, а зйомка типової ділянки поверхні шліфа в характеристичних випромінюваннях визначила його хімічну неоднорідність.

Рентгенівським дифрактометричним методом встановлено, що основними фазами сплаву є фази C_{15} і C_{14}. Крім того в сплаві містяться вторинні фази $Ni_{10}Zr_7$ та $Ni_{11}Zr_9$.

Методом потенціометричного циклування встановлено, що витримка на повітрі порошку сплаву $ZrMn_{0.5}Ni_{1.2}Cr_{0.18}A_{0.1}$ призводить до підвищення електрохімічної стабільності електродів, спресованих з цього порошку і є причиною значного покращення їх циклічної стійкості. Важливо, що покращується циклічна стійкість сплаву AB_2, легованого хромом і алюмінієм одночасно, що, зазвичай, проводять з метою підвищення циклостійкості за рахунок створення проникливих для водню стійких оксидних плівок.

Сплави з однаковим вмістом фази $Ni_{10}Zr_7$ мають однакову швидкість активації вихідних електродів. Збільшення вторинної фази $Ni_{10}Zr_7$ призводить до покращенню кінетики гідрування вихідного електроду. Витримка на повітрі порошку сплаву з підвищеним вмістом фази $Ni_{10}Zr_7$ не прискорює кінетику гідрування, однак призводить до суттєвого покращення його циклічної стійкості. При зменшенні кількості фази $Ni_{10}Zr_7$ покращення кінетики гідрування відбувається в результаті витримки порошку сплаву на повітрі.

Механізм зародження і поширення корозії сплаву без витримки і з витримкою на повітрі протягом 7 і 15 діб з наступною витримкою в 30 % розчині КОН однаковий. Згідно з дослідженнями, корозія матеріалу зароджується на міжфазній поверхні і починає поширюватися уздовж неї , що свідчить про її пітінговий характер, а поверхня самого піттінга має вигляд чешуєк.

Ключові слова: Zr-сплав, гідрування, витримка на повітрі.